


 Cite this: *RSC Adv.*, 2021, **11**, 8540

## Effect of addition of HTa to Al/PTFE under quasi-static compression on the properties of the developed energetic composite material

 Xinxin Ren, <sup>a</sup> Yuchun Li, <sup>\*a</sup> Junyi Huang, <sup>a</sup> Jiaxiang Wu, <sup>a</sup> Shuangzhang Wu, <sup>a</sup> Qiang Liu, <sup>\*a</sup> Ruiqi Wang<sup>a</sup> and Bin Feng<sup>b</sup>

To study the mechanical properties and reaction characteristics of Al/HTa/PTFE reactive materials under quasi-static compression, five types of Al/HTa/PTFE specimens with different HTa contents were prepared for quasi-static compression tests. The fracture of selected specimens was characterized by scanning electron microscopy (SEM). The quasi-static compression reaction residue underwent X-ray diffraction (XRD) phase analysis, and the chemical reaction mechanism was analyzed based on the result. As revealed from the results, the introduction of HTa significantly influenced the strength of the composites. With the increase in HTa content, the compressive strength of Al/HTa/PTFE materials first decreased and then increased. Under a HTa content of 30%, the compressive strength increased by nearly 10.6%. The microstructure shows that the HTa content in the Al/HTa/PTFE materials affects the bonding force between the metal particles and the PTFE matrix, the integrity of the PTFE matrix and the formation of PTFE bridging filaments between the deformed surfaces of the PTFE matrix, resulting in a difference in compressive strength. HTa increased the reaction duration and smoke concentration, and induced a similar white burning flame at the later phase of the reaction, with greater flame luminosity. The high temperature of the crack tip of the specimen induced the reaction of Al and PTFE and released considerable heat causing HTa to release H<sub>2</sub>, synthesized TaC, and increased the energy density, which achieved the purpose of enhancing the mechanical properties and reaction characteristics of the material.

Received 24th October 2020

Accepted 20th January 2021

DOI: 10.1039/d0ra09084k

[rsc.li/rsc-advances](http://rsc.li/rsc-advances)

## 1 Introduction

Fluoropolymer-based reactive materials are one of the most popular reactive materials, and are synthesized by mixing two or more solid materials, cold pressing and then vacuum sintering. Such types of material are inert under normal conditions, and no reaction takes places between the components. Under the action of impact, however, chemical reactions can occur to release large amounts of energy.<sup>1-4</sup> Compared with conventional insensitive explosives, Al/PTFE exhibits a higher level of energy release and better mechanical properties. Test specimens can be prepared abiding by equipment requirements and employed in air defense, anti-missile, obstacle breaking and other fields. They can cause double damage to the target based on chemical and mechanical energies. It is of high application value in military damage and other fields and has broad development prospects.<sup>5,6</sup>

In recent years, notable progress has been made on the mechanical and reaction properties of PTFE/Al reactive materials. Osborne *et al.*<sup>7</sup> studied the effect of Al particle size on the

reaction characteristics of Al/PTFE materials, and found that the sensitivity and intensity of nano-scale PTFE/Al reactions are improved. Xu *et al.*<sup>8</sup> studied the effects of Al content and strain rate on the mechanical properties of PTFE/Al materials, and found that the material has a strain rate effect and the strength of the material is maximum when the Al content is 35%. Li *et al.*<sup>9</sup> studied PTFE/Al/CuO prepared from nano-Al and nano-CuO, and found that PTFE is both an oxidizing agent and a reducing agent, and excess Al also reacts with CuO and releases a large amount of heat. Huang *et al.*<sup>10</sup> studied the mechanical properties of PTFE/Al/Fe<sub>2</sub>O<sub>3</sub> composites. It is found that as the content of PTFE increases, the strength of the material increases and only materials with high PTFE content will react. To enhance the mechanical properties of the material and increase the kinetic energy, the researchers have also added tungsten (W) and nickel (Ni) high-density metal elements to the PTFE/Al composite material.<sup>11-15</sup> Metal hydrides are a new type of energetic materials. Researches have shown that dehydrogenation takes places, when metal hydrides are involved in the reaction. Besides, the decomposition products, metal and H<sub>2</sub>, can react with other substances, thereby generating a lot of energy.<sup>16</sup> Therefore, researchers have added titanium hydride (TiH<sub>2</sub>) and zirconium hydride (ZrH<sub>2</sub>) to the PTFE/Al composite to increase the reaction energy level, and studied the

<sup>a</sup>College of Field Engineering, PLA Army Engineering University, Nanjing, 210007, China. E-mail: liyuchunmail@163.com

<sup>b</sup>China Huayin Ordnance Test Center, Huayin, Shanxi, China



preparation process, mechanical properties, reaction performance and energy release performance of the material.<sup>17–19</sup> However, the existing research has not considered adding metal hydride which can increase energy density and material density at the same time.

Because HTa contains high hydrogen content and does not decompose during the preparation of Al/HTa/PTFE composite materials.<sup>20</sup> The previous researches have shown that metal hydrides quickly decompose and release hydrogen when they reach a certain temperature. The product hydrogen continues to participate in the reaction to generate remarkable high reaction calorific value. So it can be used as a high-energy additive to increase the energy density of the material. On the one hand, the density is as high as  $15.1 \text{ g cm}^{-3}$ , which can increase kinetic energy. Accordingly, this study introduced HTa into the Al/PTFE reactive material first, prepared five types of Al/HTa/PTFE specimens with different HTa contents for quasi-static compression experiment, and combined the scanning electron microscope (SEM) to observe the interior microstructure of the specimens. The reaction energy of the materials were measured by an adiabatic bomb calorimeter and the reaction processes was analyzed based on the X-ray diffraction (XRD) of the reaction residue. According to the experimentally achieved results, the effect of HTa on the mechanical properties and reaction mechanism of Al/PTFE reactive material were analyzed.

## 2 Experimental section

### 2.1 Materials and specimen preparation

**Materials.** The mean sizes of the three raw materials were Al: 1  $\mu\text{m}$  (Shanghai), HTa: 8  $\mu\text{m}$  (Ningxia) and PTFE: 25  $\mu\text{m}$  (Shanghai).

**Specimen preparation.** According to the chemical equilibrium ratio (26.5 wt%/73.5 wt%), the mass fractions of the Al and PTFE in each type of specimens were proportioned, and varying contents of HTa particles were added as additive. The specific configuration of each type of granular composites is listed in Table 1.

First, the three powder materials were weighed and mixed by the proportion in the table. In order to form a suspension, add an appropriate amount of absolute ethanol to the mixed materials and stirred with an electric mixer for 20 min. Subsequently, the mixed suspension was placed in a vacuum oven at 60  $^{\circ}\text{C}$  to dry for 48 h. Then the mixtures were sieved to produce uniform powders, which were cold pressed under hydraulic press to make cylindrical specimen of  $\Phi 10 \text{ mm} \times 10 \text{ mm}$  (the

**Table 1** Components and theoretical material density (TMD), realistic material density (RMD) of the Al/HTa/PTFE granular composites

Type	PTFE/wt%	Al/wt%	HTa/wt%	TMD/(g cm <sup>-3</sup> )	RMD/(g cm <sup>-3</sup> )
1 <sup>#</sup>	73.5	26.5	0	2.31	2.28
2 <sup>#</sup>	69.8	25.2	5	2.42	2.37
3 <sup>#</sup>	66.2	23.8	10	2.53	2.46
4 <sup>#</sup>	58.8	21.2	20	2.79	2.71
5 <sup>#</sup>	51.5	18.5	30	3.10	3.02

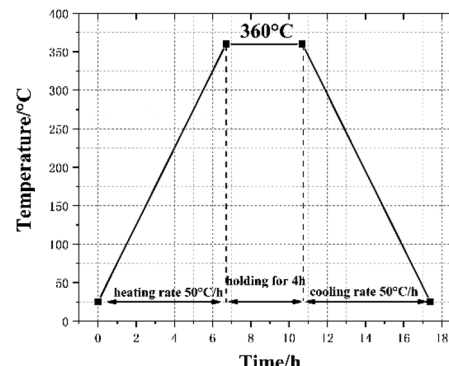


Fig. 1 The temperature history of the sintering cycle.

pressure and holding time respectively set to 240 MPa and 20 s). Lastly, the cylindrical specimens were sintered under vacuum at 360  $^{\circ}\text{C}$ . Fig. 1 presents the time history of the sintering cycle. In brief, increase to 360  $^{\circ}\text{C}$  at a heating rate of  $50 \text{ }^{\circ}\text{C h}^{-1}$  and holding for 4 h, then cooling to ambient temperature at the rate of  $50 \text{ }^{\circ}\text{C h}^{-1}$ . Prepare three specimens for each type of materials and the sintered specimens are illustrated in Fig. 2.

### 2.2 Experimental procedures

Quasi-static compression tests of the five types of specimens were performed by exploiting a CMT5105 electrohydraulic press under a maximum loading capacity of 100 kN, the force decay rate was set to 20%, and the ambient temperature at 30  $^{\circ}\text{C}$ . The load was applied at the speed of  $6 \text{ mm min}^{-1}$  corresponding to the nominal strain rate of  $0.01 \text{ s}^{-1}$ . Prior to tests, all contact surfaces of the specimens were lubricated with petroleum jelly to reduce the wearing effect. The experiment was performed in triplicate for each type of specimens. The reaction process was recorded with a high-speed camera (FASTCAM SA-Z, Photron, Tokyo, Japan). The fracture surface of the specimens before and after quasi-static compression were observed by scanning electron microscope (S-4800 Hitachi). The reaction residue was analyzed with an X-ray diffractometer (Rigaku SmartLab 9), the test condition was 40 kV, 150 mA. The adiabatic bomb calorimetry (Parr 6300, Parr Inc., Illinois, USA) was used to measure the material's calorific value of type 1<sup>#</sup> and 5<sup>#</sup> materials.

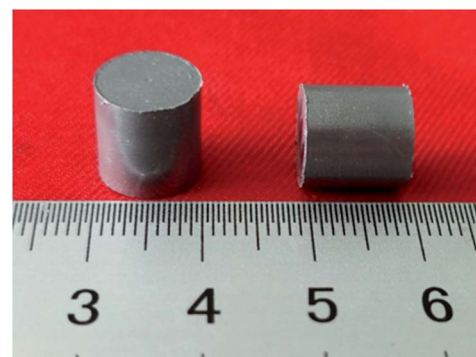


Fig. 2 The cylindrical specimens after sintered.



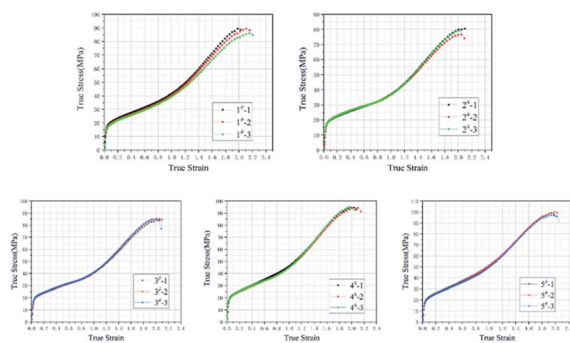


Fig. 3 Individual stress-strain curves for different types.

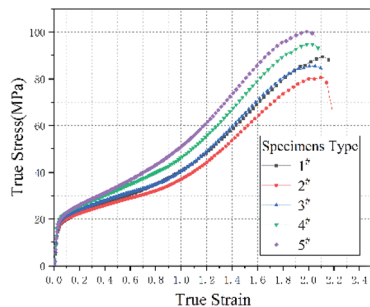


Fig. 4 Stress-strain curves of different Al/HTa/PTFE types.

### 3 Results and discussion

#### 3.1 Analysis of mechanical properties under quasi-static compression

Fig. 3 plots the quasi-static compression true stress-strain curves of type 1<sup>#</sup>, 2<sup>#</sup>, 3<sup>#</sup>, 4<sup>#</sup> and 5<sup>#</sup> specimens. The results imply that, each type of specimens undergoes three stages under quasi-static compression, *i.e.*, linear elastic stage, strengthening stage and failure stage. Fig. 4 plots the stress-strain curves of each type based on the intermediate values of each type in Fig. 3, and the corresponding mechanical performance parameters are listed in Table 2. With the increase in HTa content, the compressive strength of Al/HTa/PTFE materials decreased first and then increased. The compressive strength of Al/PTFE is obviously higher than type 2<sup>#</sup> and 3<sup>#</sup> specimens. Under the HTa content of 30% (type 5<sup>#</sup>), the compressive strength reached 99.2 MPa, 10.6% higher than Al/PTFE.

Fig. 5 shows the microstructure diagram of the fracture of type 1<sup>#</sup>, 2<sup>#</sup>, and 5<sup>#</sup> specimens before and after quasi-static compression. Fig. 5a–c compared the local internal

microstructure characteristics of type 1<sup>#</sup>, type 2<sup>#</sup> and type 5<sup>#</sup> specimens before quasi-static compression in the case of the same magnification. From the picture of microstructure diagram, the bonding surface between metal and PTFE will change if the content of HTa in the specimens are different. Compared with type 1<sup>#</sup> specimens, there are more voids on the bonding surface of metal particles and PTFE matrix in type 2<sup>#</sup> specimens. This leads to a decrease in the effective bonding surface and a decrease in bonding force. However, in the type 5<sup>#</sup> specimens, the gap between the Al particles and the PTFE matrix is smaller than that in the 1<sup>#</sup> specimen, resulting in a tighter fit and greater bonding force. On the other hand, 2<sup>#</sup> specimens have more cavities in the PTFE matrix compared with 1<sup>#</sup> specimens, which leads to lower integrity. However, 5<sup>#</sup> specimen PTFE matrix has fewer cavities than 1<sup>#</sup> specimen, resulting in a significant increase in integrity.

Fig. 5d and e compare the local interior microstructures characteristics of the type 2<sup>#</sup>, 3<sup>#</sup> specimens after quasi-static compression. It can be seen that the metal particles and PTFE matrix of the type 2<sup>#</sup> specimens are peeled and deformed, and the PTFE filaments formed was less. However, in the type 5<sup>#</sup> specimens, the morphology of the metal particles basically did not change, and a network of overlapping PTFE filaments were formed between the deformed layers. This is consistent with proposal of Brown,<sup>21</sup> and Cai *et al.*<sup>22,23</sup> that during the compression process of the specimen, the specimen nucleates from the stress concentration and forms stable filaments in the principal stress direction, which can disperse energy and passivate the crack tip by bridging the fracture surface to prevent crack propagation.

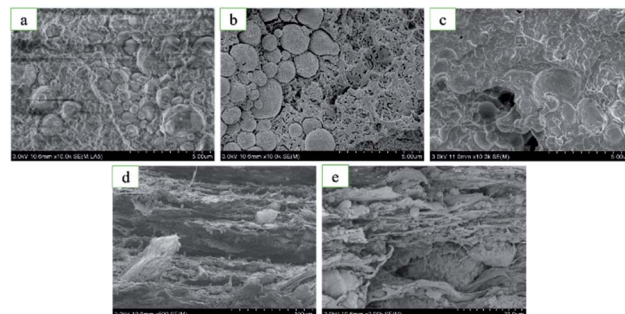


Fig. 5 Materials microstructure: (a) type 1<sup>#</sup> specimens before quasi-static compression. (b) Type 2<sup>#</sup> specimen before quasi-static compression. (c) Type 5<sup>#</sup> specimens before quasi-static compression. (d) Type 2<sup>#</sup> specimens after quasi-static compression. (e) Type 5<sup>#</sup> specimens after quasi-static compression.

Table 2 Mechanical parameters of Al/HTa/PTFE reactive materials under quasi-static loading

Type	Yield strength/MPa	Elasticity modulus/MPa	Compressive strength/MPa	Failure strain
1 <sup>#</sup>	14.54	697.61	89.67	2.13
2 <sup>#</sup>	14.67	616.46	79.15	2.01
3 <sup>#</sup>	15.85	716.90	85.09	2.00
4 <sup>#</sup>	16.03	894.51	94.91	2.01
5 <sup>#</sup>	15.01	770.23	99.20	1.96



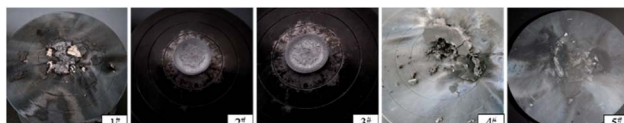


Fig. 6 The state of type 1<sup>#</sup>–5<sup>#</sup> specimens after quasi-static compression.

This indicates that the content of HTa in Al/HTa/PTFE materials affects the bonding force between the metal particles and the PTFE matrix, the integrity of the PTFE matrix and the formation of PTFE bridging filaments between the deformed surfaces of the PTFE matrix, which together lead to the difference in compressive strength.

### 3.2 Reaction characteristics under quasi-static compression

The results of the quasi-static compression test of type 1<sup>#</sup>, 2<sup>#</sup>, 3<sup>#</sup>, 4<sup>#</sup> and 5<sup>#</sup> specimens are presented in Fig. 6. To be specific, the type of 1<sup>#</sup>, 4<sup>#</sup>, and 5<sup>#</sup> specimens were all reacted. However, the specimens of type 2<sup>#</sup> and 3<sup>#</sup> failed after loading, and the appearance of the failed specimens displayed crack. The specific quasi-static compression reaction process was that as the universal materials testing machine continued to be loaded, the specimen was deformed first; when the stress increased to the compressive strength, the specimen emitted several crisp sound, and then the specimen suddenly reacted violently, accompanied by a bright fire and black smoke.

The quasi-static compression reaction phenomenon of the specimens with different proportions was also different (Fig. 7). As revealed from the comparison of 1<sup>#</sup> reaction phenomenon to 4<sup>#</sup> and 5<sup>#</sup> reaction phenomenon, the type 1<sup>#</sup> specimens had only yellow flame, while the reaction specimens with HTa (4<sup>#</sup>, 5<sup>#</sup>) showed yellow flame at the early phase of reaction, and similar gas combustion of white bright flame appeared at the later phase of reaction. With the increase in HTa content, the white flame turned out to be more prominent, and multiple fires occurred; the concentration of the smoke of the reaction product was also more concentrated, obviously different from the reaction phenomenon of the PTFE/Al specimens. Moreover, it is indicated that the average reaction duration of the test specimens increased with the increase of HTa content. Besides, type 1<sup>#</sup> specimens had the most violent reaction, and the reaction was completed rapidly from the beginning to the end, and the reaction time was the shortest in each type.

Table 3 indicates the significant difference in the reaction conversion rate and duration of reaction. The main reason for the difference in reaction rate can be mainly attributed to the fact that the compressive strength of 2<sup>#</sup> and 3<sup>#</sup> was low, causing the material did not absorb sufficient energy to reach the reaction threshold when the quasi-static compression failed. However, with the increase of HTa content, the compressive strength of type 4<sup>#</sup>, 5<sup>#</sup> specimens were restored and reached higher than Al/PTFE specimens. Moreover, the specimen could absorb enough energy to induce a reaction when it failed to compress.

According to Fig. 6 and 7, as the HTa content increased, the residue left by the reaction turned increasingly less and the

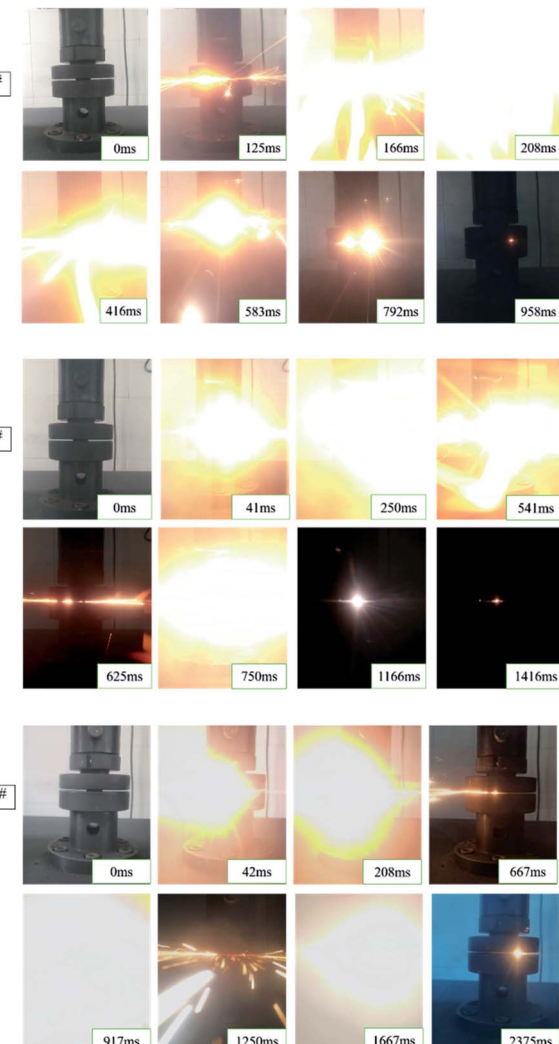


Fig. 7 Reaction processes of different types of specimens under quasi-static compression.

smoke turned out to be thicker. This can be attributed to the deflagration of the gas when HTa activated and released H<sub>2</sub> and participated in the reaction, causing the reactants to fly. Besides, the duration of reaction extended with the increase of HTa content, the analysis holds that is due to Al/PTFE reacts first and the exothermic heat of the reaction will activate HTa. Furthermore, hydrogen will be released from HTa and burn at high temperatures.

Table 3 The reaction rate and reaction time of five types of specimens under quasi-static compression

Type	Reaction rate/%	Duration of reaction/s
1 <sup>#</sup>	100	0.958
2 <sup>#</sup>	0	0
3 <sup>#</sup>	0	0
4 <sup>#</sup>	100	1.416
5 <sup>#</sup>	100	2.375



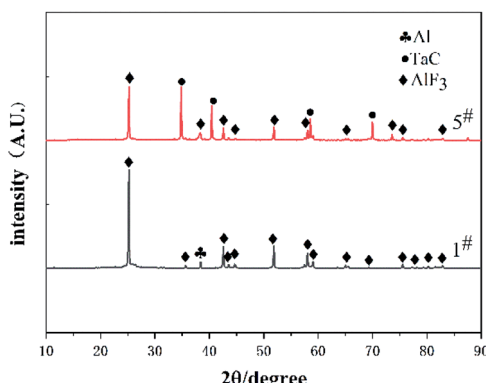


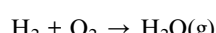
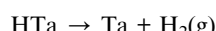
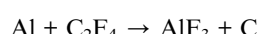
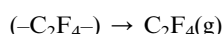
Fig. 8 XRD results of reaction residues.

In addition, as revealed from the calorimetric results, the calorific value of Al/HTa/PTFE powder is higher than that of Al/PTFE powder under the identical volume. The calorific value of Al/HTa/PTFE powder with 30% HTa content is nearly  $10.27 \text{ MJ kg}^{-1}$ , expressed as  $3.1837 \times 10^4 \text{ MJ m}^{-3}$  by volume ratio. The calorific value of Al/PTFE powder is nearly  $12.476 \text{ MJ kg}^{-1}$ , denoted as  $2.8857 \times 10^4 \text{ MJ m}^{-3}$  by volume ratio. Accordingly, the introduction of HTa under the same volume can generate more heat of reaction of the materials. Thus, in practice, the addition of HTa can increase the density and facilitate armor penetration, as well as elevate the energy release level of the reactive materials.

### 3.3 Analysis of reaction mechanism under quasi-static compression

To gain insights into the chemical reaction mechanism of composite materials, X-ray diffraction analysis was conducted on the reaction residues of type 1<sup>#</sup> and 5<sup>#</sup> specimens. The XRD results are presented in Fig. 8. The result indicate that AlF<sub>3</sub> was formed in the reaction residues of type 1<sup>#</sup> and 5<sup>#</sup> specimens. What's more, TaC was also found in the type 5<sup>#</sup> specimens reaction residue. Furthermore, there was no diffraction peak of HTa in the XRD pattern of 5<sup>#</sup>. This means that HTa was fully involved in the reaction.

Given the composition of reaction products, the possible chemical reactions process of Al/HTa/PTFE can be concluded below:



Feng *et al.*<sup>24</sup> proposed a crack-induced mechanism of Al/PTFE under quasi-static compression. Given the study, the

reaction mechanism of Al/HTa/PTFE can be inferred, *i.e.*, when the stress reaches the compressive strength under quasi-static compression, the cracks starts to propagate with accelerating speed. The temperature rises sharply at the crack tip, which cause the formation of a local hot spot along the direction of cracks extension. Therefore, PTFE and Al were reacted in the early stage of the reaction, and released a lot of heat. In the late phase, the heat stimulates HTa to generate Ta and release H<sub>2</sub> rapidly. Moreover, H<sub>2</sub> reacts with O<sub>2</sub> to produce water vapor (H<sub>2</sub>O) and release considerable heat. The product Ta reacts with C to form TaC.

## 4 Conclusions

The mechanical properties and reaction characteristics of Al/HTa/PTFE specimens with different contents of HTa were investigated under quasi-static compression. The main conclusions are drawn below:

(1) With the increase of HTa content, the compressive strength of the reactive materials first decreased and then increased. Under the HTa content of 30%, the compressive strength increased by nearly 10.6%. The phenomenon was explained by the together influence of bonding force between the metal particles and the PTFE matrix, the integrity of the PTFE matrix, and the filaments formation of the PTFE matrix in different content of HTa.

(2) The different reaction rates and reaction phenomena are attributed to the different compressive strength and the different content of hydrogen. Calorimetry results prove that adding HTa can increase the reaction energy of Al/PTFE materials.

(3) The local hot spot at the crack tip induced a chemical reaction between Al and PTFE which stimulate HTa to decompose Ta, H<sub>2</sub> and generate H<sub>2</sub>O, TaC.

## Conflicts of interest

The authors declare that there is no conflict of interest regarding the publication of this paper.

## Acknowledgements

The acknowledgements financial support from the National Natural Science Foundation of China (General Program. Grant No. 51673213) and the National Natural Science Foundation of China (Grant No. 51803235) are gratefully acknowledged.

## Notes and references

- Y. Li, Z. C. Wang, *et al.*, Experimental Study on Reaction Characteristics of PTFE/Ti/W Energetic Materials under Explosive Loading, *Materials*, 2016, **9**(11), 936.
- M. T. Rose, D. W. Doll and J. R. Hodgson, Reactive material enhanced projectiles and related methods, *US Pat.*, 20160209187, 2009.



3 W. Mock, Impact Initiation of Rods of Pressed Polytetrafluoroethylene (PTFE) and Aluminum Powders, *AIP Conf. Proc.*, 2006, **845**, 1097–1100.

4 H. F. Wang, Y. F. Zheng, Q. B. Yu, *et al.*, Impact-induced initiation and energy release behavior of reactive materials, *J. Appl. Phys.*, 2011, **110**(7), 074904.

5 G. Chao, Y. X. Dong and W. Maimaitituersun, Microscale Simulation on Mechanical Properties of Al/PTFE Composite Based on Real Microstructures, *Materials*, 2016, **9**(7), 590.

6 E. M. Hunt and M. L. Pantoya, Impact sensitivity of intermetallic nanocomposites: a study on compositional and bulk density, *Intermetallics*, 2010, **18**(8), 1612–1616.

7 D. T. Osborne and M. L. Pantoya, Effect of Al Particle Size on the Thermal Degradation of Al/Teflon Mixtures, *Combust. Sci. Technol.*, 2007, **179**(8), 1467–1480.

8 S. L. Xu, Study on the mechanical properties of PTFE/Al energetic reaction materials, PhD thesis, National University of Defense Technology, 2010.

9 X. Y. Li, Study on Preparation and Reaction Characteristics of Fluorine-containing Nano Thermite, PhD thesis, Nanjing University of Science and Technology, 2016.

10 J. Y. Huang, X. Fang, Y. C. Li, *et al.*, The Mechanical and Reaction Behavior of PTFE/Al/Fe<sub>2</sub>O<sub>3</sub> under Impact and Quasi-Static Compression, *Adv. Eng. Mater.*, 2017, 3540320.

11 J. Zhou, H. E. Yong, H. E. Yuan, *et al.*, Quasi-static Compression Properties and Impact Energy Release Characteristics of Al/PTFE/W Reactive Materials, *Chin. J. Energ. Mater.*, 2017, **25**(11), 903–912.

12 H. X. Wang, Y. C. Li, B. Feng, *et al.*, Compressive Properties of PTFE/Al/Ni Composite Under Uniaxial Loading, *J. Mater. Eng. Perform.*, 2017, **26**, 2331–2336.

13 C. Ge, W. Maimaitituersun, Y. Dong, *et al.*, A Study on the Mechanical Properties and Impact-Induced Initiation Characteristics of Brittle PTFE/Al/W Reactive Materials, *Materials*, 2017, **10**(5), 452.

14 L. Qiao, J. Tu, L. J. Zhao, *et al.*, Influence of particle size grading on strength of Al/W/PTFE composite, *Ordnance Mater. Sci. Eng.*, 2014, (6), 17–21.

15 J. Cai, V. F. Nesterenko, K. S. Vecchio, *et al.*, The influence of metallic particle size on the mechanical properties of PTFE-Al-W powder composites, *Appl. Phys. Lett.*, 2008, **92**(3), 031903.

16 Y. Yang, F. Zhao, Z. Yuan, *et al.*, On the combustion mechanisms of ZrH<sub>2</sub> in the double-base propellant, *Phys. Chem. Chem. Phys.*, 2017, **19**, 32597–32604.

17 Z. S. Yu, X. Fang, Y. C. Li, *et al.*, Investigation on the Reaction Energy, Dynamic Mechanical Behaviors, and Impact-Induced Reaction Characteristics of PTFE/Al with Different TiH<sub>2</sub> Percentages, *Materials*, 2018, **11**(10), 2008.

18 Z. S. Yu, X. Fang, Z. R. Gao, *et al.*, Mechanical and Reaction Properties of Al/TiH<sub>2</sub>/PTFE under Quasi-Static Compression, *Adv. Eng. Mater.*, 2018, 1800019.

19 J. Zhang, Y. C. Li, J. Y. Huang, *et al.*, The effect of al particle size on thermal decomposition, mechanical strength and sensitivity of Al/ZrH<sub>2</sub>/PTFE composite, *Def. Technol.*, 2020, DOI: 10.1016/j.dt.2020.05.013.

20 P. Ren, H. Y. Ma, Y. W. Cheng, *et al.*, Study on Recovery Process of Waster Tantalum Target and Its Application, *Nonferrous Met.*, 2018, **04**, 71–74.

21 E. N. Brown and D. M. Dattelbaum, The role of crystalline phase on fracture and microstructure evolution of polytetrafluoroethylene (PTFE), *Polymer*, 2005, **46**(9), 3056–3068.

22 J. Cai, Properties of heterogeneous energetic materials under high strain, high strain rate deformation, PhD thesis, AAI3274695, ProQuest Dissertation and thesis, 2007, ISBN: 97805491341072007.

23 J. Cai, S. M. Walley, R. J. A. Hunt, *et al.*, High-strain, high-strain-rate flow and failure in PTFE/Al/W granular composites, *Mater. Sci. Eng., A*, 2008, **472**(1–2), 308–315.

24 B. Feng, X. Fang, Y. C. Li, *et al.*, An initiation phenomenon of Al-PTFE under quasi-static compression, *Chem. Phys. Lett.*, 2015, **637**, 38–41.

